THE ASTROPHYSICAL JOURNAL, 458:363–370, 1996 February 10


# INTERSTELLAR DUST ABSORPTION FEATURES IN THE INFRARED SPECTRUM OF HH 100-IR: SEARCHING FOR THE NITROGEN COMPONENT OF THE ICES

D. C. B. WHITTET,[1] R. G. SMITH,[2] A. J. ADAMSON,[3] D. K. AITKEN,[2] J. E. CHIAR,[1] T. H. KERR,[3,4]
P. F. ROCHE,[5] C. H. SMITH,[2] AND C. M. WRIGHT[2,6]
*Received 1995 June 12; accepted 1995 August 15*

## ABSTRACT

We present observations of solid-state absorption features due to water ice, CO ice, and silicate dust in the spectrum of the bright infrared source (IRS 1) associated with the Herbig-Haro nebula HH 100 in the R Coronae Australis dark cloud. These absorptions are shown to arise predominantly in the molecular cloud rather than in circumstellar matter associated with the infrared source itself, which we deduce to be a pre–main-sequence star obscured by ~25 mag of visual extinction. In common with other lines of sight, the spectra indicate the presence of distinct hydrogen-rich (polar) and hydrogen-poor (nonpolar) phases in the ice toward HH 100-IR. The nonpolar phase is dominated by CO. The strength of the solid CO feature at 4.67 $\mu$m suggests that as much as ~40% of all CO in the line of sight may be in the solid phase. Our data show a lack of significant absorption at 4.62 $\mu$m that might arise in CN-bearing molecules formed by energetic processing of the mantles.

A previous report of structure in the profile of the 3 $\mu$m water-ice feature in HH 100-IR that might be attributed to the N-H resonance in condensed ammonia at ~2.96 $\mu$m is not confirmed. The abundance ratio $NH_3$:$H_2O$ in the ices is found to be no more than ~8%, which is probably insufficient to account for the 3.3–3.6 $\mu$m "ice-band wing" in terms of ammonium hydrate. However, we propose that the wing might be explained by hydrates containing other bases in addition to ammonia. Further progress is likely to require new laboratory data for appropriate ice mixtures.

*Subject headings:* dust, extinction — infrared: ISM: lines and bands — ISM: molecules — line: identification — stars: individual (HH 100) — stars: pre–main-sequence

## 1. INTRODUCTION

Nitrogen is among the most abundant elements likely to be present in interstellar ices, yet its chemistry is poorly constrained by available observational data. Models for mantle growth by accretion and surface catalysis (d'Hendecourt, Allamandola, & Greenberg 1985) predict distinct phases of ice mantle growth on grain surfaces in interstellar clouds: regions in which atomic H is of comparable abundance with C, N, and O in the gas phase produce hydrogen-rich ices dominated by $H_2O$, $NH_3$, and $CH_4$ or $CH_3OH$, whereas regions in which H to $H_2$ conversion is essentially complete produce hydrogen-poor ices containing CO, $O_2$, $N_2$, and $CO_2$. Infrared spectroscopy has provided observational evidence in support of this general scenario: in particular, studies of the solid CO feature at 4.67 $\mu$m provide strong evidence for distinct polar ($H_2O$-dominated) and nonpolar (CO-dominated) phases (e.g., Tielens et al. 1991; Chiar et al. 1994). However, a convincing observational identification has yet to be made for abundant N-bearing species predicted in either polar or nonpolar ices.

$N_2$ is a homonuclear molecule and thus lacks an infrared signature in its pure state. The fundamental N ≡ N stretching vibration may in principle be observed through perturbations of neighbors when $N_2$ is embedded in a host matrix; however, the band strength is intrinsically weak, and, as this resonance occurs at 4.3 $\mu$m, it is in any case unobservable from ground-based or airborne platforms due to strong telluric $CO_2$ absorption. $NH_3$ on the other hand, should be quite easily detectable. Spectra of laboratory $H_2O$:$NH_3$ ice mixtures exhibit a narrow absorption feature near 2.96 $\mu$m, due to the N-H stretching resonance, superposed on the broader O-H water-ice feature centered at 3.05 $\mu$m (Hagen, Tielens, & Greenberg 1983a). In addition, a broad, shallow absorption occurs at longer wavelengths (3.2–3.6 $\mu$m) due to the O-H stretching resonance in water molecules in ammonium hydrate groups (HOH...$NH_3$, where ... represents the hydrogen bond). This latter feature has been suggested as an identification for the long-wavelength "shoulder" or "wing" seen in the observed profile of the interstellar ice feature (Merrill, Russell, & Soifer 1976; Hagen, Tielens, & Greenberg 1983b; van de Bult, Greenberg, & Whittet 1985; Schutte 1988), which would require an $NH_3$ abundance ~10%–20% that of $H_2O$. If this identification is correct, then the observed ice profile is effectively a blend of O-H resonances in water (HOH...$OH_2$) and ammonium hydrate (HOH...$NH_3$), centered at ~3.05 $\mu$m and ~3.4 $\mu$m, respectively.

However, the N-H stretch feature has proved elusive and its detection problematical (Knacke et al. 1982; Knacke & McCorkle 1987; Smith, Sellgren, & Tokunaga 1989; Smith, Sellgren, & Brooke 1993). In particular, Smith et al. (1989) report sensitive observations of the N-H stretch region in the spectra of two deeply embedded young stars (BN and AFGL 989), and deduce an $NH_3/H_2O$ ratio in the ices of no more than ~2%. Such a low abundance of $NH_3$ might be surprising

[1] Department of Physics, Applied Physics and Astronomy, Rensselaer Polytechnic Institute, Troy, NY 12180.
[2] Department of Physics, Australian Defense Force Academy, University of New South Wales, Campbell, ACT 2600, Australia.
[3] Department of Physics and Astronomy, University of Central Lancashire, Preston PR1 2HE, England, UK.
[4] Present address: Department of Chemistry, University of Nottingham, Nottingham, England, UK.
[5] Department of Astrophysics, University of Oxford, Oxford OX1 3RH, England, UK.
[6] Present address: Max-Planck-Institut für Extraterrestrische Physik, Postfach 1603, D-85740 Garching, Germany.

on theoretical grounds, as $NH_3$ is predicted to be the primary carrier of N in the polar ices according to the model of d'Hendecourt et al. (1985). An abundance of $\sim 2\%$ is well below that required for a significant contribution by ammonium hydrate to the long-wavelength wing. It may also conflict with chemical models for hot molecular cores (Charnley, Tielens, & Millar 1992; Walmsley & Schilke 1993), which attribute high observed gas-phase $NH_3$ abundances in these regions to evaporation of icy grain mantles. However, Graham & Chen (1991) have subsequently reported possible detections of the N-H feature in young stars associated with Herbig-Haro objects. Comparison of the Smith et al. and Graham & Chen results suggests that the $NH_3$ abundance might be a strong function of environment.

In this paper, we present observations of dust features in HH 100-IR, with emphasis on the quest to identify the important molecular form(s) of nitrogen in the solid phase. HH 100-IR is the most highly obscured of the sources observed by Graham & Chen (1991). We review the nature of the object and its line of sight in § 2 below. Our spectra provide coverage of the principal features of silicate dust (§ 3), water ice (§ 4), and nonpolar (CO-rich) mantles (§ 6). The data allow us to investigate the evolutionary state of the ices and to determine the abundance of the solid-phase $H_2O$ and CO. We place quantitative limits on the abundance of two nitrogen-bearing species, ammonia (§ 5) and isonitriles (§ 6), the latter by means of the C≡N resonance near 4.6 $\mu$m. The implications of these results are discussed in the final section.

## 2. THE NATURE AND ENVIRONMENT OF HH 100-IR

An intense infrared source associated with the Herbig-Haro nebula HH 100 was first detected by Strom, Strom, & Grasdalen (1974). This source[7] is located at

$$\text{R.A.} = 18^{\text{h}}58^{\text{m}}28^{\text{s}}.3\ , \quad \text{Decl.} = -37°02'27''\ (1950)\ ,$$

approximately 25″ northeast of the optical nebula but coincident with a peak in line emission from dense molecular gas (Anglada et al. 1989). HH 100-IR is highly variable in the near-infrared (Axon et al. 1982). It is a strong far-infrared source (Cohen et al. 1984; Reipurth et al. 1993), although it is not listed in the Point Source Catalog of the *Infrared Astronomical Satellite* due to confusion with other bright far-infrared sources in the region. It is generally accepted that HH 100-IR is a member of a newly formed star cluster embedded in the R Coronae Australis (R CrA) dark cloud (Strom et al. 1974; Cohen et al. 1984; Wilking, Taylor, & Storey 1986). The presence of hydrogen line emission (Br$\alpha$: Beck, Fischer, & Smith 1991; Pf$\beta$: this paper, § 6) and the absence of photospheric CO overtone absorption (this paper, § 4) argue against interpretation as an obscured late-type field star seen through the molecular cloud by chance alignment. Polarization measurements indicate the presence of a circumstellar disk (Bastien & Ménard 1990) and the object appears to drive a bipolar flow (Anglada et al. 1989), strengthening its identification as the source of excitation for the Herbig-Haro nebula.

One may attempt to explain the observed properties of HH 100-IR in terms of either an intrinsically cool "protostellar" object or a more evolved pre–main-sequence star with high extinction. At the distance of the cloud ($\sim 130$ pc; Marraco & Rydgren 1981), a visual extinction $A_V > 10$ would be required to explain the absence of a visible counterpart if the source were a typical pre–main-sequence star of moderate mass. In fact, the molecular line observations of Anglada et al. (1989) imply a total opacity equivalent to $A_V \sim 30$ in the line of sight. The double-peaked form of the spectral energy distribution of HH 100-IR (Cohen et al. 1984) is suggestive of a reddened star with a dust shell rather than a protostar. In comparison with other infrared sources associated with Herbig-Haro objects, the absolute far-infrared (1300 $\mu$m) flux of HH 100-IR is low relative to its bolometric luminosity by at least a factor of 2 (see Reipurth et al. 1993), indicating that it is no longer deeply embedded in accreting material. We conclude that the weight of evidence favors interpretation as a pre–main-sequence star situated behind a molecular core. On the assumption that it illuminates the Herbig-Haro nebula, the optical spectrum of the star may be studied in reflected light: Cohen et al. (1986) conclude that HH 100-IR unmistakably scatters the chromospheric spectrum of a strong emission-line T Tauri star.

It is possible to further constrain the visual extinction of the object. Since normal stellar intrinsic colors show only small variation in $H-K$ with respect to spectral type and luminosity class (e.g., Bessel & Brett 1988), $H-K$ may be used to estimate $E_{H-K}$ and hence $A_V$ in sources lacking spectral type information (e.g., Chen & Graham 1993), assuming an appropriate extinction law. The relation may be stated

$$A_V = kE_{H-K} = k[(H-K) - (H-K)_0]\ , \qquad (1)$$

where $k$ is a constant and subscript 0 denotes the intrinsic value. The mean extinction laws tabulated by Martin & Whittet (1990) imply $k \simeq 16.1$ (diffuse ISM) and $k \simeq 12.9$ ($\rho$ Oph dark cloud), results which differ somewhat from the "canonical" value of $k = 12$ derived by Elias (1978a, b) and subsequently assumed by several authors (e.g., Tanaka et al. 1990, 1994; Chen & Graham 1993). As the dust in the R CrA dark cloud may resemble that in the $\rho$ Oph dark cloud more closely than that in the diffuse interstellar medium (ISM) (e.g., Vrba, Coyne, & Tapia 1981), we adopt $k = 13 \pm 1$. Assuming $(H-K)_0 = 0$ (appropriate to an A0 star), and $H-K = 3.5$ (Table 1 of Chen & Graham 1993) we obtain $A_V < 46$ for HH 100-IR, where the limiting value arises because the near-infrared colors are affected by circumstellar excess emission. However, Strom et al. (1974) argue that HH 100-IR is intrinsically similar to the pre–main-sequence star R CrA, which has low extinction. On this basis, we obtain $E_{H-K} \simeq 1.9$ for HH 100-IR (the difference in $H-K$ colors given by Chen & Graham for HH 100-IR and R CrA) and thus $A_V \simeq 25$. This is comparable with the value of $\sim 30$ estimated from molecular line observations (Anglada et al. 1989), suggesting that HH 100-IR lies behind most of the molecular material in the line of sight. We show below (§ 3) that it is also consistent with the depth of the silicate feature observed in HH 100-IR.

Gas-phase molecular line observations provide constraints on physical conditions along the line of sight. The region has been mapped in $C^{18}O$ by Harju et al. (1993) and in $NH_3$ by Anglada et al. (1989). HH 100-IR lies toward clump A2 of the "R CrA core" (Fig. 1 of Harju et al.) and is coincident with a southern subpeak in the $NH_3$ emission within that clump (Fig. 11 of Anglada et al.). The clump has mass $\sim 2\ M_\odot$, spatial extent $\sim 0.05$ pc, density $n(H_2) \sim 2 \times 10^4$ cm$^{-3}$ and temperature $\sim 15$ K. The column density of molecular hydrogen is estimated to be $N(H_2) \simeq 3 \times 10^{22}$ cm$^{-2}$ (Anglada et al. 1989) from the $NH_3$ observations. If we assume that the total hydro-

[7] We adopt the designation HH 100-IR; the source is also known as CrA IRS 1 and TS 2.6.

gen column density $N(H) = N(HI) + 2N(H_2)$ is closely correlated with visual extinction, as is the case in regions of lower density (Roche & Aitken 1984; Whittet 1992), then we estimate $N(H) \simeq 1.9 \times 10^{21} A_V \simeq 5 \times 10^{22}$ cm$^{-2}$ toward HH 100-IR, in good agreement with the molecular line observations if most of the hydrogen is in molecular form.

Evidence for absorption features due to dust in the infrared spectrum of HH 100-IR was first reported by Whittet & Blades (1980), who detected the 3.05 $\mu$m feature of water ice. Observations at higher resolution in the same spectral region by Graham & Chen (1991) suggest the presence of fine structure in the water-ice profile, as discussed in § 1, notably an absorption at 2.97 $\mu$m interpreted as evidence for $NH_3$. If $NH_3$ is indeed present in the ice mantles on grains in this line of sight, it may contribute to the observed long-wavelength (3.3–3.6 $\mu$m) wing. Recently, a detection of solid CO absorption at 4.67 $\mu$m toward HH 100-IR was reported by Tanaka et al. (1994), indicating that at least some of the icy grain material in the line of sight is in the form of nonpolar condensates at temperatures less than 20 K.

## 3. SILICATES

HH 100-IR was observed on 1986 April 29, with the University College London cooled grating spectrometer on the Anglo-Australian Telescope (AAT) at Siding Spring Observatory, New South Wales, Australia. The detector was a helium-cooled 25-element Si:As array, and the spectral range 8–13 $\mu$m was covered at a mean resolution of 0.23 $\mu$m through a 4″.3 aperture. The resulting spectrum is shown in Figure 1.

The characteristic silicate absorption profile centered at 9.7 $\mu$m is clearly seen in the spectrum. Attempts were made to fit this profile with various models, using "Trapezium" and "$\mu$ Cephei" silicate emissivity functions and a blackbody continuum, as described by Roche & Aitken (1984). Pure absorption models gave consistently better fits than models that assume a combination of circumstellar emission and foreground absorption. The best fit (illustrated in Fig. 1) was obtained with the Trapezium profile in absorption and a 380 K blackbody continuum. The resulting peak optical depth in the feature is $\tau_{9.7} = 1.21 \pm 0.05$. Previous studies of other lines of sight indicate that the Trapezium emissivity curve generally gives best fits to sources obscured by dust in molecular clouds and star-forming regions, whereas the $\mu$ Cephei curve gives best fits to sources obscured by diffuse-cloud dust or circumstellar matter around late-type stars (Roche & Aitken 1984, 1985; Whittet et al. 1988). Our spectrum of HH 100-IR is consistent with this pattern.

The lack of a strong circumstellar component in the 9.7 $\mu$m profile toward HH 100-IR encourages us to believe that the optical depth of the feature may be used to obtain an independent estimate of the visual extinction. Silicates are ubiquitous in the ISM at all levels of density and appear to be well mixed with gas and with other forms of dust. In diffuse regions within a few kpc of the Sun, $\tau_{9.7}$ and $A_V$ display a high degree of linear correlation described by the equation $A_V \simeq (18.5 \pm 1.0)\tau_{9.7}$ (Whittet 1992; Roche & Aitken 1984). It is unclear how well this result describes the correlation in molecular clouds: the observations of Whittet et al. (1988) show a markedly greater degree of scatter in $A_V/\tau_{9.7}$ for the Taurus cloud compared with the diffuse ISM. Adoption of the diffuse-cloud correlation yields $A_V = 22 \pm 3$ for HH 100-IR. In summary, an adopted value of $A_V = 25 \pm 4$ seems consistent with this and other estimates (§ 2) and their associated random and systematic errors.

## 4. WATER ICE

Observations of HH 100-IR in the spectral region of the 3 $\mu$m ice feature were made on 1988 April 24, using the cooled grating spectrometer CGS2 on the United Kingdom Infrared Telescope (UKIRT), Mauna Kea Observatory, Hawaii. The detector was a nitrogen-cooled 7-element InSb array. To obtain good definition of the continuum on either side of the broad solid state feature, the $K$-band atmospheric window was covered from 2.2 to 2.5 $\mu$m in addition to the $L$-band window from 2.8 to 4.0 $\mu$m. The aperture size was 5″ and the mean spectral resolution was 0.005 $\mu$m. Wavelength calibration was achieved with reference to an argon lamp and is good to one resolution element. Standard chopping and beamswitching techniques were used. Spectral scans of HH 100-IR were ratioed with corresponding scans of a standard star, BS 6084 (spectral type B1 III), to provide flux calibration and calculation of telluric features. Both program and standard stars were observed at airmasses in the range 1.75–1.85. The resulting spectrum, shown in Figure 2, has been Hanning smoothed to improve signal-to-noise ratio, which results in a 20% degradation in resolution. Data points near 3.3 $\mu$m have

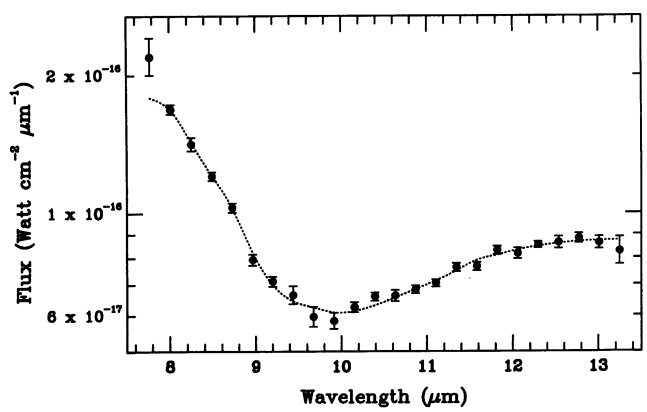


FIG. 1.—Flux spectrum of HH 100-IR from 8 to 13 $\mu$m (*points*), compared with the best-fitting model (*dotted curve*). The model assumes a silicate absorption profile matching the Trapezium emissivity curve (Roche & Aitken 1984) with a blackbody (380 K) continuum.

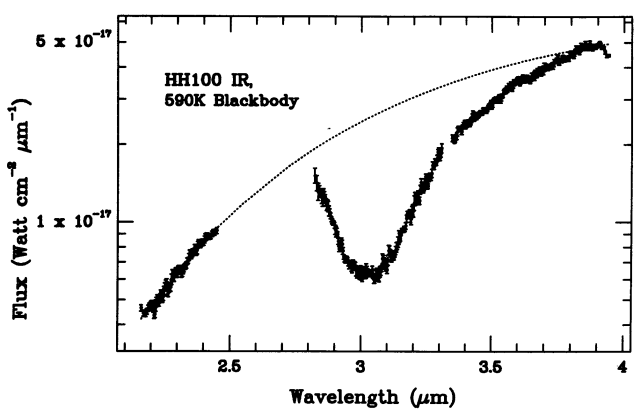


FIG. 2.—Flux spectrum of HH 100-IR from 2.2 to 4.0 $\mu$m (*points*). The adopted continuum for the ice feature (a 590 K blackbody: see text) is shown as a dotted line.

TABLE 1

OPTICAL DEPTHS, COLUMN DENSITIES, AND RELATED INFORMATION FOR ICE FEATURES OBSERVED TOWARD HH 100-IR

| Molecule | $\lambda$ ($\mu$m) | $A$[a] (cm molecule$^{-1}$) | $\Delta\nu$ (cm$^{-1}$) | $\tau_\lambda$ | $N$ (cm$^{-2}$) | $N/N(H_2O)$ (%) |
|---|---|---|---|---|---|---|
| $H_2O$ ..... | 3.05 | $2.0 \times 10^{-16}$ | 340[b] | $1.44 \pm 0.06$ | $2.4 \times 10^{18}$ | ... |
| $NH_3$ ..... | 2.96 | $1.1 \times 10^{-17}$ | 45[a] | <0.05 | $<2.0 \times 10^{17}$ | <8 |
| $NH_3$ ..... | 9.35 | $1.7 \times 10^{-17}$ | 68[a] | <0.06 | $<2.4 \times 10^{17}$ | <10 |
| XCN..... | 4.62 | $3.0 \times 10^{-17}$ | 20[c] | <0.06 | $<4.0 \times 10^{16}$ | <2 |
| CO(n)[d]..... | 4.67 | $1.0 \times 10^{-17}$ | 5[b] | $0.89 \pm 0.04$ | $4.5 \times 10^{17}$ | 19 |
| CO(b)[e]..... | 4.68 | $1.7 \times 10^{-17}$ | 13[b] | $0.22 \pm 0.06$ | $1.7 \times 10^{17}$ | 7 |

[a] Integrated absorption intensities and FWHM from laboratory data (d'Hendecourt 1984; d'Hendecourt & Allamandola 1986; Tielens & Allamandola 1987; Sandford et al. 1988; Gerakines et al. 1995).
[b] Estimated from model fits to our observations.
[c] From observational data (Tegler et al. 1995).
[d] Narrow component, nonpolar ices.
[e] Broad component, polar ices.

been omitted due to imperfect calculation of the strong telluric methane absorption feature at this wavelength.

The 2.2–2.5 $\mu$m segment of the spectrum appears featureless to within observational error and should therefore provide a reliable constraint on the continuum of the ice feature. On the long-wavelength side, the wing of the ice feature typically extends to about 3.7–3.8 $\mu$m (e.g., Willner et al. 1982). A blackbody of temperature 590 K provides an acceptable representation of the continuum in HH 100-IR, matching the 2.2–2.5 $\mu$m data well and extrapolating plausibly to longer wavelengths, as shown in Figure 2. (As reddening has been ignored, this does not imply any assumptions concerning the temperature of the source.) An optical depth spectrum of the 2.8–4.0 $\mu$m data calculated from this adopted continuum is shown in Figure 3. The peak optical depth ($\tau_{3.05}$) and the derived column density (see below) are listed with other relevant data in Table 1.

The profile of the water-ice feature (Fig. 3) lacks obvious fine structure. We attempted to fit the feature with core/mantle grain models described by Smith et al. (1989, 1993). These models assume an "MRN" power-law size distribution of silicate cores (Mathis, Rumpl, & Nordsieck 1977) and pure $H_2O$-ice mantles with variable thickness. Ice optical constants as a function of temperature are taken from Kitta & Krätschmer (1983). The best fit to our spectrum (shown in Fig. 3) is obtained with core radii in the range 0.005–0.25 $\mu$m, maximum mantle thickness 0.28 $\mu$m, and mantle optical constants for amorphous $H_2O$ ice at 23 K (model 14 of Smith et al. 1993). This model predicts a feature depth to extinction ratio of $\tau_{3.05}/A_V = 0.059$, in good agreement with our results for HH 100-IR. Models which assume optical constants for ices at higher temperatures give significantly worse fits (see Smith et al. 1989 for comparison, where fits are presented for various deeply embedded young stars). We conclude that the ices toward HH 100-IR exist at low temperature, consistent with their assumed location in the foreground molecular cloud (§ 2).

Our results for HH 100-IR, in combination with data from the literature for field stars obscured by the R CrA cloud, allow us to investigate the dependence of the ice feature on visual extinction. Previous investigators use $H-K$ as a proxy for extinction (Chen & Graham 1993; Tanaka et al. 1994; see § 2), which implicitly assumes $(H-K)_0 = 0$. The extinction is then slightly overestimated for a late-type star. However, spectral type information exists in the literature for several field stars in the R CrA cloud, and we are therefore able to use equation (1) to refine previous estimates of $A_V$. Results are listed in Table 2, and a plot of $\tau_{3.05}$ against $A_V$ appears in Figure 4. The field

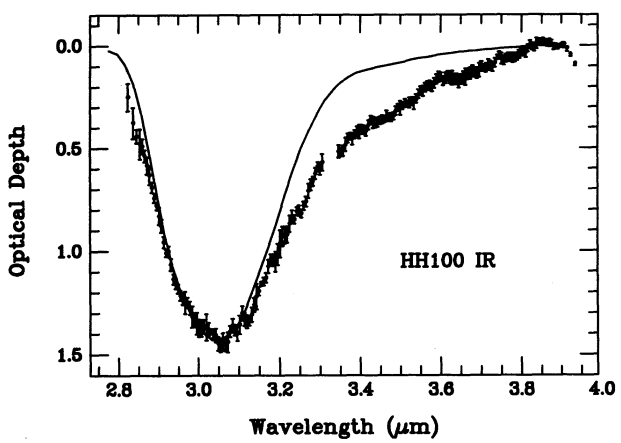


FIG. 3.—Optical depth spectrum of the ice feature in HH 100-IR, based on the data and continuum plotted in Fig. 2. The solid curve is the best-fitting model based on silicate core/ice mantle grains, using laboratory data for amorphous ice at a temperature of 23 K (Smith et al. 1993, model 14).

TABLE 2

SPECTRAL TYPES, VISUAL EXTINCTIONS, AND 3 $\mu$m ICE OPTICAL DEPTHS FOR FIELD STARS BEHIND THE R CrA CLOUD

| Source | Spectral Type | $H-K$ | $A_V$[a] | $\tau_{3.05}$ |
|---|---|---|---|---|
| TS1.8 ..... | ... | 0.40 | 5.2[b] | <0.10[c] |
| TS3.5 ..... | K-M[d] | 0.70 | 6.6 | 0.27[e] |
| TS4.1 ..... | K-M[d] | 1.41 | 15.9 | 0.85[e] |
| TS4.4 ..... | K-M[d] | 1.02 | 10.8 | 0.40[f] |
| VCT10..... | B9[g] | 0.22 | 3.2 | <0.10[c] |
| VCT30..... | A0[g] | 0.22 | 2.9 | <0.10[c] |
| VCT46..... | G7[g] | 0.35 | 3.8 | <0.05[c] |
| VCT58..... | K0 III[g] | 0.26 | 2.1 | <0.07[c] |
| VCT84..... | K1 III[g] | 0.22 | 1.6 | <0.10[c] |

[a] Assumes $A_V = 13[(H-K) - (H-K)_0]$; intrinsic colors are from Bessell & Brett 1988.
[b] Assumes $(H-K)_0 = 0$.
[c] Estimated from spectra of Chen & Graham 1993.
[d] From Tanaka et al. 1994; luminosity class III assumed.
[e] Average of values from Chen & Graham 1993 and Tanaka et al. 1994.
[f] From Tanaka et al. 1994.
[g] From Vrba et al. 1981; luminosity class V assumed unless otherwise stated.

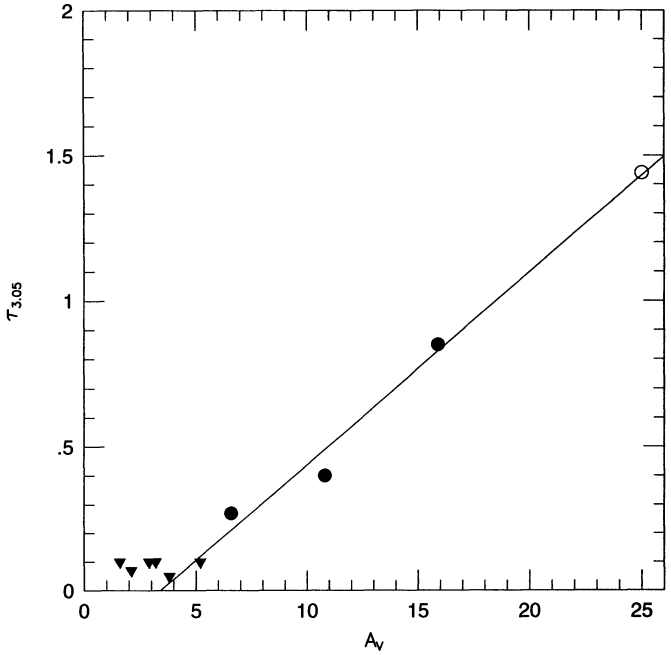


FIG. 4.—Plot of optical depth at the peak of the water-ice feature ($\tau_{3.05}$) against visual extinction ($A_V$) for the R CrA cloud. HH 100-IR is represented by an open circle. Field star data (*filled circles and triangles*) are from Table 2. The triangles denote upper limits. The solid line is the fit to the points with upper limits excluded.

stars show a pattern consistent with observations of other clouds, with nondetections below some threshold visual extinction $A_0$, and a systematic trend of increasing $\tau_{3.05}$ with $A_V$ for $A_V > A_0$ (e.g., Williams, Hartquist, & Whittet 1992). We also include HH 100-IR in the plot, using our adopted value of $A_V$ (§ 3) and $\tau_{3.05}$ from Table 1. The locus of HH 100-IR is consistent with the trend for field stars, suggesting that dust in the molecular core toward HH 100-IR is typical of the dark cloud as a whole in terms of the degree of ice deposition per unit grain mass. A least-squares fit of the relation

$$\tau_{3.05} = q(A_V - A_0) \tag{2}$$

gives slope $q = 0.066 \pm 0.006$ and intercept $A_0 = 3.4 \pm 0.3$ (ignoring upper limits but including HH 100-IR along with the field stars). This result for R CrA may be compared with data for other clouds. Interestingly, a very similar value of $A_0$ has been deduced for the Taurus dark cloud (2.6–3.3; Smith et al. 1993; Whittet et al. 1988), and that for Serpens (5–6; Eiroa & Hodapp 1989) is somewhat similar, whereas a much higher value of 10–15 (Harris, Woolf, & Reike 1978; Tanaka et al. 1990) is apparent in the $\rho$ Oph dark cloud. Differences in $A_0$ presumably arise because of variations in the ambient radiation fields (Williams et al. 1992). These results appear to suggest that R CrA, like Taurus, is a relatively quiescent cloud complex, in which internal dust is generally well shielded from radiative processing.

The column density of molecules in the ice mantles may be estimated by means of the formula

$$N = \frac{\tau \Delta v}{A}, \tag{3}$$

where $\Delta v$ ($\mathrm{cm}^{-1}$) is the full-width at half-maximum optical depth and $A$ (cm per molecule) is the integrated absorption intensity (e.g., Allamandola & Sandford 1988). Table 1 lists results for $H_2O$ and other molecules in our study of HH 100-IR. Considering the cloud as a whole, the abundance of water in the mantles at extinctions $A_V > A_0$ is given by

$$\frac{N(H_2O)}{N(H)} \simeq 2.63 \times 10^{-6} q \Delta v \tag{4}$$

(see eq. [5.1] of Whittet 1992). Using our value of $q$ from Figure 2, and $\Delta v \simeq 340$ $\mathrm{cm}^{-1}$, we obtain $N(H_2O)/N(H) \sim 6 \times 10^{-5}$. This may be compared with the cosmic abundance of oxygen, $N(O)/N(H) \sim 8.5 \times 10^{-4}$ (Anders & Grevesse 1989), suggesting that $\sim 7\%$ of the available oxygen is contained in the $H_2O$ component of the ice mantles in R CrA. The Taurus cloud yields a similar result ($\sim 10\%$; Whittet 1992), which further supports the view that the two clouds are similar in terms of the conditions governing ice deposition and desorption.

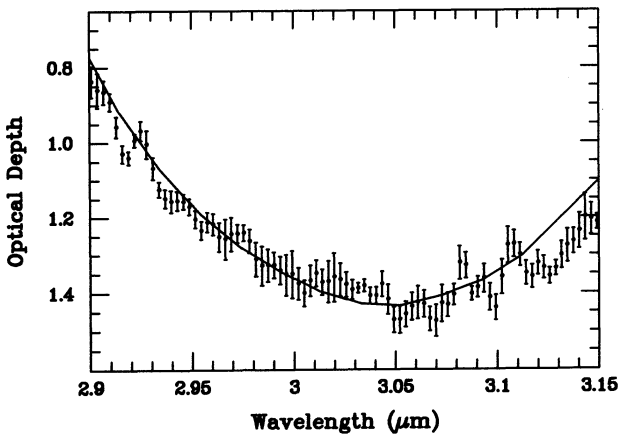


FIG. 5.—Enlargement of Fig. 3 in the 2.90–3.15 $\mu$m region, illustrating the lack of any detectable absorption associated with the N-H stretching resonance in ammonia at 2.97 $\mu$m.

## 5. AMMONIA

The spectra described in the previous sections allow us to search for the N-H stretch and umbrella modes of $NH_3$ at 2.96 and 9.35 $\mu$m, respectively. Figure 5 shows an enlargement of Figure 3 in the region of the N-H stretch. If present, the 2.96 $\mu$m feature would appear as excess absorption structure of width (FWHM) $\sim 0.04$ $\mu$m (e.g., d'Hendecourt 1984), superposed on the water-ice profile. There is clearly no such feature present in our spectrum, the data points being matched by the calculated pure water-ice profile to within observational error at this wavelength.[8] We deduce an upper limit on the optical depth and hence on the $NH_3$ column density (eq. [3]) in the ices. These results appear in Table 1.

Similarly, we find no appreciable absorption at 9.35 $\mu$m in the silicate profile (Fig. 1). In this case, the expected FWHM is $\sim 0.5$ $\mu$m (d'Hendecourt 1984). The upper limit on the $NH_3$

[8] The origin of the discrepancy between our result and that of Graham & Chen (1991) is uncertain. There is no strong telluric feature at this wavelength, and Graham & Chen argue that the feature they detect cannot be attributed to incomplete atmospheric calculation. It is possible that the spectrum of HH 100-IR varies with time, as does its broadband flux in the near-infrared, but it is unclear how this could account for the appearance or nonappearance of the N-H feature.

column density implied by this nondetection (Table 1) is similar to that based on the 2.96 $\mu$m feature: both spectra suggest that $N(NH_3) < 2 \times 10^{17}$ cm$^{-2}$ in the solid phase toward HH 100-IR.

Assuming the usual cosmic abundance ratio (Anders & Grevesse 1989), the expected total column density of nitrogen in the line of sight to HH 100-IR is deduced to be $N(N) \simeq 1.1 \times 10^{-4} N(H) \simeq 5.6 \times 10^{18}$ cm$^{-2}$. Comparing this with the results in Table 1, we conclude that $NH_3$ accounts for no more than $\sim$4% of the available nitrogen.

## 6. SOLID CO AND "XCN"

Spectroscopy of HH 100-IR in the wavelength range 4.56–4.77 $\mu$m was obtained on 1992 May 23, using the cooled grating spectrometer CGS4 on UKIRT. The detector was a nitrogen-cooled 58 × 62 InSb array, operated at 35 K with a closed-cycle cooling system. The aperture was a 3″ × 90″ slit and the chop amplitude was 20″ north–south. The 75 lines mm$^{-1}$ grating was used with the short focal length (150 mm) camera to give a spectral resolution of 0.004 $\mu$m. The spectrum was oversampled by a factor of 3. The wavelength scale was calibrated relative to an argon lamp and is accurate to $\sim$0.001 $\mu$m. Spectral scans of HH 100-IR were ratioed with corresponding scans of a standard star, BS 7194 (spectral type A2 III), to allow calculation of telluric features and provide a flux-calibrated spectrum. Both HH 100-IR and the standard star were observed at an airmass of approximately 1.95. A linear continuum was fitted to the data in the wavelength ranges 4.56–4.64 $\mu$m and 4.72–4.77 $\mu$m, and the resulting optical depth plot is shown in Figure 6.

The 4.67 $\mu$m feature of solid CO dominates the spectrum. The only other significant feature is a peak at 4.65 $\mu$m which corresponds to the Pf$\beta$ line of hydrogen. This line is present in emission in HH 100-IR, although a contribution to its intensity in Figure 6 may arise due to photospheric absorption in the A-type standard star. An unpublished spectrum of HH 100-IR obtained at lower resolution with CGS2 on UKIRT in 1988 April, ratioed with a standard star of later spectral type, confirms the reality of Pf$\beta$ emission in HH 100-IR.

The shape of the solid CO feature in Figure 6 indicates that separate polar and nonpolar ices are present, in common with

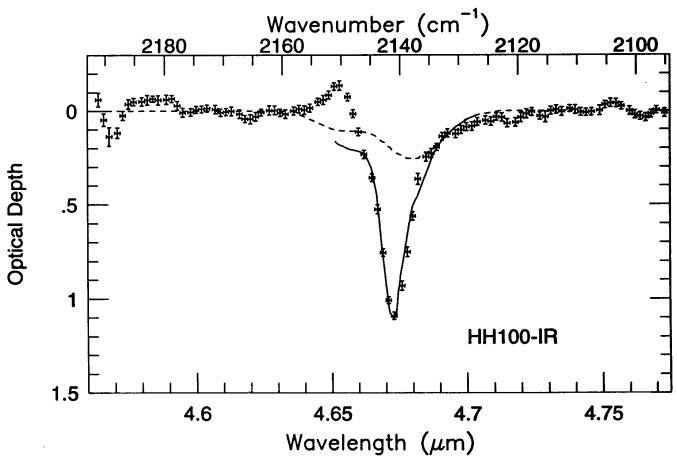


FIG. 6.—Optical depth spectrum of HH 100-IR in the region of the 4.62 $\mu$m "XCN" and 4.67 $\mu$m CO features. The continuous curve is a fit to the CO feature, based on the summation of broad and narrow components (see text). The broad component is also shown as a dashed curve.

many other lines of sight intersecting cold molecular clouds. We carried out fits to the profile using techniques described previously by Kerr, Adamson, & Whittet (1993) and Chiar et al. (1994, 1995). Laboratory spectra are fitted to the data using a $\chi^2$ minimization routine. A list of available laboratory mixtures may be found in Table 2 of Chiar et al. (1995). The routine yields fits to the broad and narrow components. Best fits to our data were obtained with CO:$H_2O$ (10:1) and $H_2O$:CO (4:1) mixtures, both at 10 K, for the narrow (nonpolar) and broad (polar) components, respectively. The resulting fit is shown in Figure 6, where the solid curve represents the combination of broad and narrow, and the dashed curve represents the broad component alone. In terms of selected mixture, this fit is identical to that found by Chiar et al. (1995) for field stars behind the Taurus dark cloud.

Optical depth and column density information are given in Table 1, with the broad and narrow components treated separately. The total solid CO column density, $N(CO) \simeq 6.2 \times 10^{17}$ cm$^{-2}$, is $\sim$25% of the solid $H_2O$ column density. These results are used by Chiar et al. (1995) in an investigation of the intercorrelation of $N(CO)$, $N(H_2O)$, and $A_V$ in several dark clouds, and the reader is referred to that paper for further discussion. We note here that HH 100-IR follows the general trend of Taurus field stars in the correlation diagrams.

Assuming that dust and molecular gas are well mixed in the ISM, the total CO column density may be estimated from the silicate optical depth:

$$N_{\rm total}(CO) \simeq (1.4 \times 10^{18}) \tau_{9.7} \quad (5)$$

(Whittet & Duley 1991). Our result, $\tau_{9.7} = 1.21$ (§ 3), leads to a value of $N_{\rm total}(CO) \simeq 1.7 \times 10^{18}$ cm$^{-2}$. Comparing this with the total solid-state CO column density (Table 1), we obtain an estimate of the depletion:

$$\delta(CO) = \frac{N_{\rm dust}(CO)}{N_{\rm total}(CO)} \simeq 0.36 , \quad (6)$$

i.e., some 30%–40% of the CO in the line of sight to HH 100-IR is frozen onto grains. This is comparable with the highest values found in dense clouds such as Serpens and Taurus, and much greater than is typical of the environments of young stars (Whittet & Duley 1991; Chiar et al. 1994, 1995).

We have also searched our spectrum (Fig. 6) for evidence of the broad feature centered at 4.62 $\mu$m, detected in several young stellar objects (Lacy et al. 1984; Tegler et al. 1995) and attributed to C≡N resonances in an unidentified organic molecule ("XCN"). Candidates for XCN include isonitriles, such as $CH_3NC$, and the cyanate ion $OCN^-$ (Larson et al. 1985; Tielens & Allamandola 1987; Grim & Greenberg 1987). XCN is not detected in our spectrum, although we cannot entirely exclude the presence of a weak feature of optical depth $\sim$0.05 (similar to that found by Tegler et al. 1995 in the embedded star Elias 18). However, the implied column density of nitrogen in CN bonds toward HH 100-IR (Table 1) is in any case very low, accounting for no more than about 1% of the total N abundance (§ 5). As XCN is believed to be produced by energetic processing of ices containing $NH_3$ or $N_2$ (Lacy et al. 1984; Tegler et al. 1995), its nondetection in HH 100-IR is consistent with other evidence presented in this paper, in particular the strength of the nonpolar solid CO feature. Tegler et al. find that the XCN feature is strong only toward sources with $\tau_{4.67}$(nonpolar)/$\tau_{3.05} < 0.4$, i.e., only in situations where

volatile nonpolar mantles are relatively weak or absent. For HH 100-IR, $\tau_{4.67}(\text{nonpolar})/\tau_{3.05} \simeq 0.62$.

## 7. WHERE IS THE NITROGEN?

Several lines of evidence presented in the previous sections indicate that the ices in the molecular cloud that obscures HH 100-IR are in a pristine state and have not been thermally or radiatively processed to a significant degree:

1. The water-ice and solid CO features are best fit with cold, unannealed mixtures.
2. The solid CO feature is dominated by nonpolar CO-rich ices, which exist only at low temperatures ($< 30$ K).
3. The ratios $N(H_2O)/A_V$, $N(CO)/A_V$, and $N(CO)/N(H_2O)$ are characteristic of the quiescent dark cloud environment, as observed toward field stars behind the Taurus cloud (Chiar et al. 1995).
4. The XCN feature, a signature of radiatively processed ices, is weak or absent.

Solid-phase nitrogen in the line of sight is thus expected to exist only in "primary" ices, such as $NH_3$ and $N_2$, rather than evolved ices produced by energetic processing. In this section, we discuss the significance of the limit we have placed on the $NH_3$ abundance and suggest some alternative carriers of nitrogen in the ices.

A key to the problem may lie in the identity of the 3.3–3.6 $\mu$m ice band wing. There are at least two strong arguments in favor of the proposed identification with ammonium hydrate. First, it is evident from moderate-resolution observations of the wing profile in HH 100-IR (§ 4) and other sources (e.g., Smith et al. 1989; Allamandola et al. 1992) that the wing absorption is quasi-continuous and not easily resolvable into discrete structure (structure does exist, but it makes only a minor contribution to the total equivalent width of the feature). This argues against an identification with a superposition of CH absorptions in a variety of organic molecules. Ammonium hydrate absorption would naturally account for the width and continuous nature of the wing. Second, Smith et al. (1993) have shown that both the wing and the principal water-ice feature at 3.05 $\mu$m have the same threshold extinction (see eq. [2]), indicating that their carriers form and survive under closely similar conditions. Again, this is naturally explained by a hydrate model, in which $H_2O$ and $NH_3$ are intimately mixed, whereas there is no reason to suppose that the variety of organic molecules needed to produce a range of CH absorptions in the 3.3–3.6 $\mu$m region would share this property.

As previously discussed, the primary objection to the ammonium hydrate identification of the wing is the nondetection of the N-H feature at 2.96 $\mu$m. It is worthwhile to examine the significance of this result in more detail. An $N(NH_3)/N(H_2O)$ ratio of $\leq 8\%$ is consistent with our observations; Smith et al. (1989) have argued for a more stringent limit ($\leq 2\%$), but Hagen et al. (1983a) conclude from laboratory data that the 2.96 $\mu$m feature is no longer discernible as a separate feature for $NH_3$ concentrations below $\sim 10\%$. Improved signal-to-noise ratio may not therefore increase the probability of detection. If we allow an $NH_3$ concentration of up to $\sim 8\%$–$10\%$, we are close to the low end of the range (10%–20%) required to explain the depth of the wing (Hagen et al. 1983a; van de Bult et al. 1985; Schutte 1988). Hagen et al. pointed out that the role of $NH_3$ in the hydrate can also be played by other strong bases. Candidates include many nitrogen-bearing molecules such as $NH_2OH$, $H_2CNH$, $HCONH_2$, and $CH_3NH_2$. Collectively, such molecules may make a contribution to the wing, even if, individually, they are unlikely to have appreciable abundance in primary ices. Some may be formed only by energetic processing, and it may be important that Smith et al. (1989) found the wing to be deeper relative to the principal feature in lines of sight where the 3 $\mu$m profile is best fit with *annealed* ices (compare, for example, spectra of Mon R2 IRS3 and Elias 16 in Smith et al. 1989). We therefore suggest that the wing might be explained by ices containing $H_2O$ and a mixture of bases. Little spectroscopic information is currently available to test this hypothesis (although Hagen et al. 1983a find structure in spectra of laboratory ice mixtures containing methylamine, $CH_3NH_2$, that has no counterpart in the astronomical data). It would be valuable to investigate the spectroscopic properties of a range of suitable mixtures in the laboratory.

Finally, we turn our attention to the nonpolar ices. Womack, Ziurys, & Wyckoff (1992) conclude that gas-phase nitrogen in dense clouds is mostly in the form of $N_2$. In the absence of an efficient desorption mechanism, it is likely that much of the $N_2$ may condense out onto grains within the lifetime of a cloud; similar arguments have been made for CO (e.g., Williams 1985), which indeed has an observed depletion of up to about 40% (§ 6). There are thus good reasons to expect a significant presence of $N_2$ in the nonpolar ices, consistent with theoretical prediction (d'Hendecourt et al. 1985). Tegler et al. (1995) suggest that $N_2$ is the most important source of nitrogen for the production of CN-bearing molecules in processed regions. Laboratory investigations of irradiated $CO:N_2$ mixtures may provide a suitable test.

This research was partially funded by the NASA Long-Term Space Astrophysics program (grant number NAGW 3144). We are grateful to the Panel for the Allocation of Telescope Time for the award of observing time on the AAT and UKIRT, and to John Graham for helpful comments.

## REFERENCES

Allamandola, L. J., & Sandford, S. A. 1988, in Dust in the Universe, ed. M. E. Bailey & D. A. Williams (Cambridge: Cambridge Univ. Press), 229
Allamandola, L. J., Sandford, S. A., Tielens, A. G. G. M., & Herbst, T. M. 1992, ApJ, 399, 134
Anders, E., & Grevesse, N. 1989, Geochim. Cosmochim. Acta, 53, 197
Anglada, G., Rodriguez, L. F., Torrelles, J. M., Estalella, R., Ho, P. T. H., Canto, J., Lopez, R., & Verdes-Montenegro, L. 1989, ApJ, 341, 208
Axon, D. J., Allen, D. A., Bailey, J., Hough, J. H., Ward, M. J., & Jameson, R. F. 1982, MNRAS, 200, 239
Bastien, P., & Ménard, F. 1990, ApJ, 364, 232
Beck, S. C., Fischer, J., & Smith, H. A. 1991, ApJ, 383, 336
Bessell, M. S., & Brett, J. H. 1988, PASP, 100, 1134
Charnley, S. B., Tielens, A. G. G. M., & Millar, T. J. 1992, ApJ, 399, L71
Chen, W. P., & Graham, J. A. 1993, ApJ, 409, 319
Chiar, J. E., Adamson, A. J., Kerr, T. H., & Whittet, D. C. B. 1994, ApJ, 426, 240
———. 1995, ApJ, 455, 234
Cohen, M., Dopita, M. A., & Schwartz, R. D. 1986, ApJ, 307, L21
Cohen, M., Schwartz, R. D., Harvey, P. M., & Wilking, B. A. 1984, ApJ, 281, 250
d'Hendecourt, L. B. 1984, Ph.D. thesis, Univ. Leiden
d'Hendecourt, L. B., & Allamandola, L. J. 1986, A&AS, 64, 453
d'Hendecourt, L. B., Allamandola, L. J., & Greenberg, J. M. 1985, A&A, 152, 130
Eiroa, C., & Hodapp, K. W. 1989, A&A, 210, 345
Elias, J. H. 1978a, ApJ, 224, 453

Elias, J. H. 1978b, ApJ, 224, 857
Gerakines, P. A., Schutte, W. A., Greenberg, J. M., & van Dishoeck, E. F. 1995, A&A, 296, 810
Graham, J. A., & Chen, W. P. 1991, AJ, 102, 1405
Grim, R. J. A., & Greenberg, J. M. 1987, ApJ, 321, L91
Hagen, W., Tielens, A. G. G. M., & Greenberg, J. M. 1983a, A&AS, 51, 389
———. 1983b, A&A, 117, 132
Harju, J., Haikala, L. K., Mattila, K., Mauersberger, R., Booth, R. S., & Nordh, H. L. 1993, A&A, 278, 569
Harris, D. H., Woolf, N. J., & Reike, G. H. 1978, ApJ, 226, 829
Kerr, T. H., Adamson, A. J., & Whittet, D. C. B. 1993, MNRAS, 262, 1047
Kitta, K., & Krätschmer, W. 1983, A&A, 122, 105
Knacke, R. F., & McCorkle, S. M. 1987, AJ, 94, 972
Knacke, R. F., McCorkle, S., Puetter, R. C., Erickson, E. F., & Krätschmer, W. 1982, ApJ, 260, 141
Lacy, J. H., Baas, F., Allamandolla, L. J., Person, S. E., McGregor, P. J., Lonsdale, C. J., Geballe, T. R., & van de Bult, C. E. P. 1984, ApJ, 276, 533
Larson, H. P., Davis, D. S., Black, J. H., & Fink, U. 1985, ApJ, 299, 873
Marraco, H. G., & Rydgren, A. E. 1981, AJ, 86, 62
Martin, P. G., & Whittet, D. C. B. 1990, ApJ, 357, 113
Mathis, J. S., Rumpl, W., & Nordsieck, K. H. 1977, ApJ, 217, 425
Merrill, K. M., Russell, R. W., & Soifer, B. T. 1976, ApJ, 207, 763
Reipurth, B., Chini, R., Krugel, E., Kreysa, E., & Sievers, A. 1993, A&A, 273, 221
Roche, P. F., & Aitken, D. K. 1984, MNRAS, 208, 481
———. 1985, MNRAS, 215, 425
Sandford, S. A., Allamandola, L. J., Tielens, A. G. G. M., & Valero, G. J. 1988, ApJ, 329, 498
Schutte, W. 1988, Ph.D. thesis, Univ. Leiden
Smith, R. G., Sellgren, K., & Brooke, T. Y. 1993, MNRAS, 263, 749
Smith, R. G., Sellgren, K., & Tokunaga, A. T., 1989, ApJ, 344, 413
Strom, K. M., Strom, S. E., & Grasdalen, G. L. 1974, ApJ, 187, 83
Tanaka, M., Nagata, T., Sato, S., & Yamamoto, T. 1994, ApJ, 430, 779
Tanaka, M., Sato, S., Nagata, T., & Yamamoto, T. 1994, ApJ, 352, 724
Tegler, S. C., Weintraub, D. A., Rettig, T. W., Pendleton, Y. J., Whittet, D. C. B., & Kulesa, C. A. 1995, ApJ, 439, 279
Tielens, A. G. G. M., & Allamandola, L. J. 1987, in Physical Processes in Interstellar Clouds, ed. G. E. Morfill & M. Scholer (Dordrecht: Reidel), 333
Tielens, A. G. G. M., Tokunaga, A. T., Geballe, T. R., & Baas, F. 1991, ApJ, 381, 181
van de Bult, C. E. P. M., Greenberg, J. M., & Whittet, D. C. B. 1985, MNRAS, 214, 289
Vrba, F. J., Coyne, G. V., & Tapia, S. 1981, ApJ, 243, 489
Walmsley, C. M., & Schilke, P. 1993, in Dust and Chemistry in Astronomy, ed. T. J. Millar & D. A. Williams (Cambridge: Cambridge Univ. Press), 37
Whittet, D. C. B. 1992, Dust in the Galactic Environment (Bristol: Institute of Physics Publishing)
Whittet, D. C. B., & Blades, J. C. 1980, MNRAS, 191, 309
Whittet, D. C. B., Bode, M. F., Longmore, A. J., Adamson, A. J., McFadzean, A. D., Aitken, D. K., & Roche, P. F. 1988, MNRAS, 233, 321
Whittet, D. C. B., & Duley, W. W. 1991, A&A Rev., 2, 167
Wilking, B. A., Taylor, K. N. R., & Storey, J. W. V. 1986, AJ, 92, 103
Williams, D. A. 1985, QJRAS, 26, 463
Williams, D. A., Hartquist, T. W., & Whittet, D. C. B. 1992, MNRAS, 258, 599
Willner, S. P., et al. 1982, ApJ, 253, 174
Womack, M., Ziurys, L. M., & Wyckoff, S. 1992, ApJ, 393, 188